Supporting Information

Proszynski et al. 10.1073/pnas.0910391106

SI Text

Cell Culture. C2C12 cells were obtained from American Type Culture Collection (ATCC, CRL-1772). Cells were cultured for five or fewer passages in DME containing 20% fetal calf serum supplemented with glutamine, penicillin, streptomycin, and Fungizone. Cells were trypsinized and replated onto 8-well Permanox chamber slides (Nalge Nunc International, 177445) for histological studies or 8-well glass chamber slides (Nalge Nunc International, 155409) for time-lapse imaging. Before plating, slides were coated with 10 μg/mL solution of laminin 111 (Invitrogen, 23017–015) in L-15 medium supplemented with 0.2% NaHCO3, incubated overnight at 37 °C, and aspirated immediately before plating cells. To induce cell fusion, growth media was replaced with fusion media containing 2% horse serum in DMEM supplemented with glutamine, penicillin, streptomycin, and Fungizone. For mechanical detachment of myotubes (11), cells were incubated with 0.2% saponin in DME media supplemented with 2% BSA for 4–8 min at 37 °C.

For primary cultures, mononucleated cells were dissociated from limb muscle of neonatal mice and plated on Matrigel-coated dishes for expansion in DME supplemented with 10% horse serum, 10% FBS, penicillin/streptomycin, and fungizone. The next day, cells were trypsinized and plated on EHS laminin (10 mg/mL, Invitrogen) coated Permanox chamber slides. Myoblasts were grown to confluency and switched to DME plus 5% horse serum with penicillin, streptomycin and TTX (1.5 mg/mL) to induce fusion and block spontaneous contractions. Cells were incubated at 5% CO_2 for 7 days before staining.

Immunostaining. For immunostaining, cells were fixed with 1–4% PFA or ice-cold acetone and washed with PBS. Nonspecific staining was blocked with 2% BSA and 2% goat serum in PBS plus 0.1% Triton X-100 before overnight incubation with primary antibodies. Monoclonal antibodies against vinculin (V4505), β-actin (A1978), talin (T3287), and non-muscle myosin IIA (M8064) were obtained from Sigma-Aldrich. Rabbit anti paxilin antibody (600701) was obtained from Biolegend. Rabbit anti-Arp2 (sc-15389) was from Santa Cruz; rabbit anti-SrcP416 (2109) was from Cell Signaling; rabbit anti-Tks5 (09–403) was from Millipore; rabbit anti-NCK (06–288) was from Upstate Cell Signaling Solutions; mouse anti-cortactin (610049) was from BD Transduction; rat anti-integrin β1 (MAB1997) was from R&D Systems; rabbit anti-dynamin (D9900–50) was from US Biological; anti-laminin β2 was a gift from the lab of R. Timpl (Max Planck-Institute for Biochemistry, Martinsried, Germany). Monoclonal antibodies to utrophin (MANCHO3 clone 8A4) and beta-dystroglycan (MANDAG2 clone 7D11) were obtained from the Developmental Stuides Hybridoma Bank developed under the auspices of the National Institute of Child Health and Human Development and maintained by The University of Iowa, Department of Biological Science, Iowa City, IA 52242. Anti-LL5β, anti-laminin 111 and anti-laminin α5 were produced in our laboratory. Phalloidin, used to visualize F-actin, was conjugated to Alexa Fluor 488 or Alexa Fluor 660 (Molecular Probes). AChRs were labeled with α-bungarotoxin conjugated to Alexa Fluor 488 or 568 (Molecular Probes). Primary antibodies were detected with Alexa Fluor 568 or 488–coupled goat secondary antibodies (Molecular Probes).

Microscopy. Epifluorescence images of fixed cells were collected on an Axio Imager Z1 microscope (Carl Zeiss MicroImaging, Inc.) fitted with a cooled charge-coupled device (CCD) camera (Carl Zeiss MicroImaging, Inc.) and PLAN-NEO FLUAR 40×/1.3 oil objective. Multiple time point observations of individual AChR aggregates were collected on a Nikon ECLIPSE TE 2000-E microscope (Nikon) equipped with a Hamamatsu 1394 ORCA-ERA camera (Hamamatsu Photonics Inc.) and PLAN APO 40×/0.95 DIC M/N2 objective. Confocal images were obtained using Fluoview1000 equipped with Plan Apo 100×, 1.45 NA or 40×, 1.3 NA objective lenses. Images were analyzed with NIS-Elements AR 3.0 software (Nikon) and edited with Adobe Photoshop version 8.0.

Interference reflection images (IRM) were collected using a Axio Imager Z1 microscope (Carl Zeiss MicroImaging, Inc.) microscope equipped with Zeiss neutral density filter (424931–0001-000) to isolated the 488-nm line of the arc source. Myoblasts were seeded and fused onto carbon-coated CC2 glass chamberslides (Nalge Nunc International, 154941). Single-plane images were collected using a cooled charge-coupled device (CCD) camera Axio Cam MRm (Carl Zeiss MicroImaging, Inc.).

In Vivo Experiments. Wild-type mouse pups were injected with 2 μL (10^8 PFU) adenovirus encoding β-actin-GFP into *Tibialis anterior* muscle. Five to six days later animals were anesthetized, perfused with PFA and the extracted tissue was incubated for 10 min in 4% PFA and washed intensively in PBS and stained with BTX conjugated to Alexa Fluor 568 to visualize AChR. The tissue was mounted in Fluoromount (Sigma, F4680–25 mL) and imaged at the confocal microscope. All animal studies have been approved by the authors' institutional review boards.

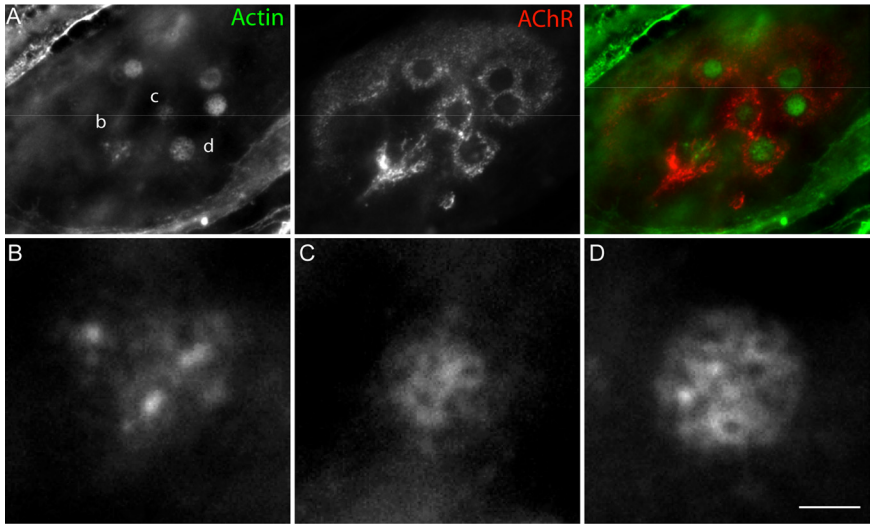

Fig. S1. Actin-rich structures that occupy perforations in AChR clusters are composed of smaller subunits. (*A*) C2C12 cells were stained with phalloidin and BTX. (*B–D*) Labeled structures are shown at higher magnification. (Scale bar, 2 μm.)

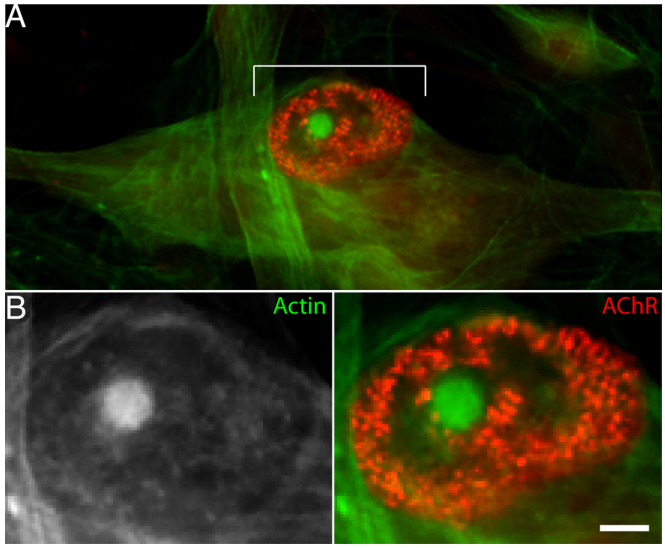

Fig. S2. Actin-rich structures in primary myotubes. (*A*) Myotubes derived from embryonic myoblasts were stained with phalloidin and BTX. Actin-rich structures are present in perforations in the AChR clusters. (*B*) Shows higher magnification from *A*. (Scale bar, 5 μm.)

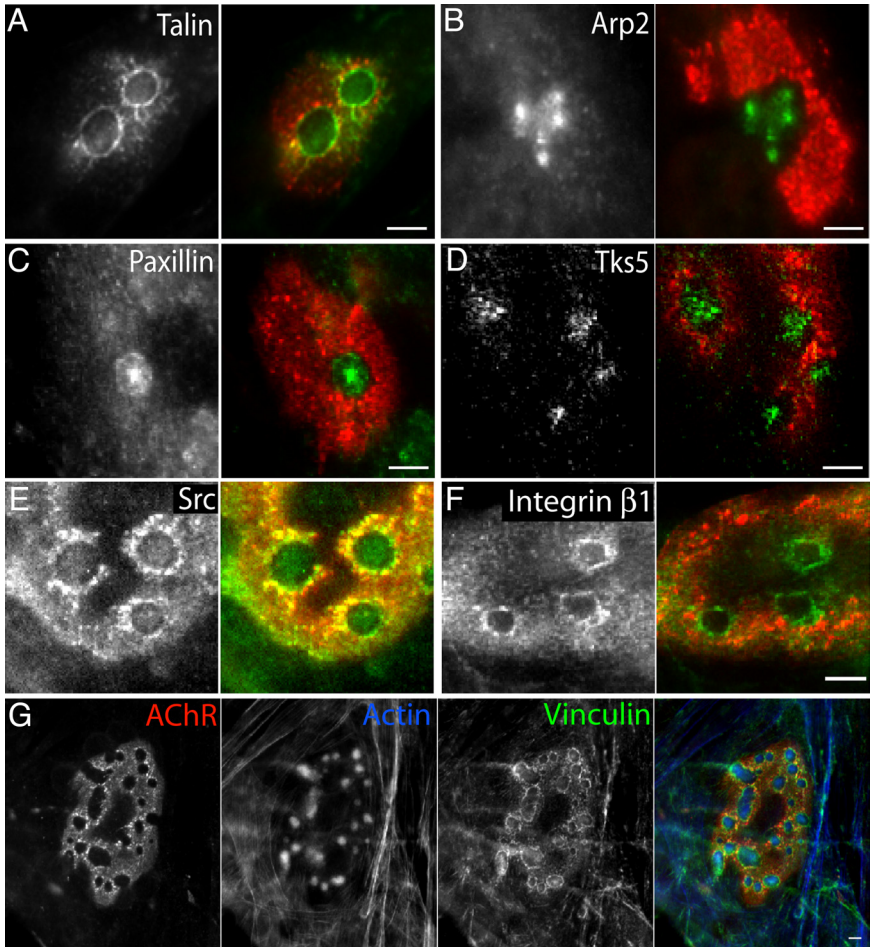

Fig. S3. Components of synaptic podosomes. (*A–F*) C2C12 myotubes stained with BTX (red) and antibodies to indicated components (green) talin (*A*), Arp2 (*B*), paxillin (*C*), Tks5 (*D*), Src (*E*), or integrin β1 (*F*). (*G*) Triple-labeling with BTX (red), phalloidin (actine, blue) and anti-vinculin antibody (green). (Scale bar, 5 μm.)

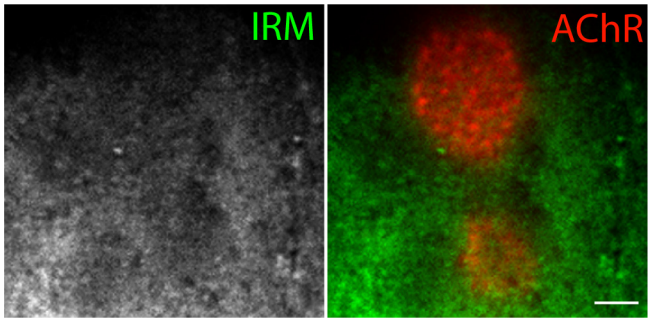

Fig. S4. Adhesion of C2C12 myotubes to substratum revealed by internal reflection microscopy (IRM). Immature AChR clusters lie within a broadly adhesive region. (Scale bar, 5 μm.)

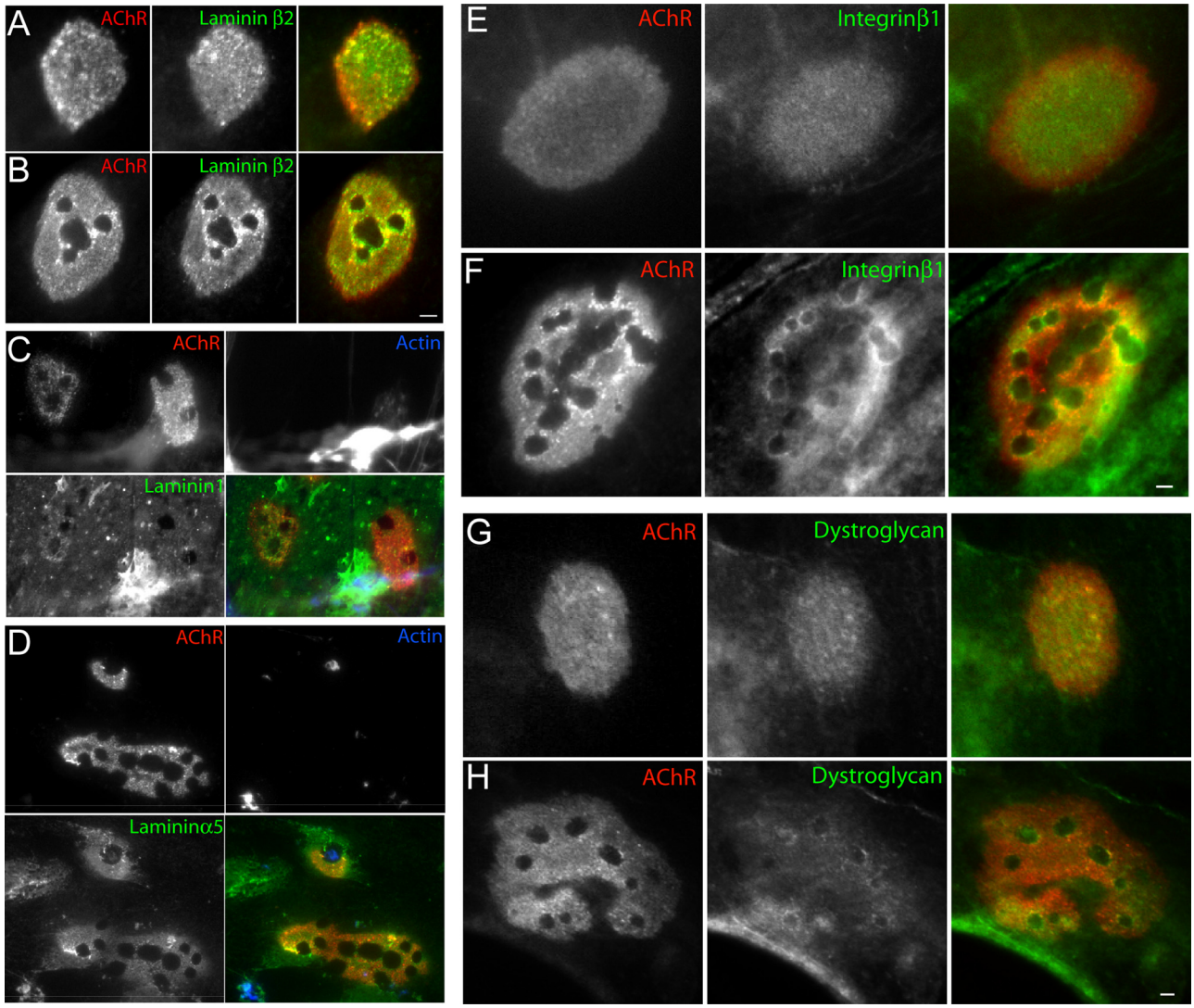

Fig. S5. Remodeling of laminins at podosomes. (*A*) Laminin β2 is distributed underneath the AChRs. After podosomes are formed it is displaced from underneath podosomes (*B*). (*C* and *D*) Mechanical removal of cells and podosomes did not affect pattern of laminin staining at perforations in AChR clusters. C2C12 myotubes were treated with saponin at 37 °C and Triton X-100 after fixation, then stained for laminin 1 (*C*) or laminin α5 (*D*). Laminins were depleted from sites of podosomes. (*E*–*H*) Similarly, transmembrane laminin receptors integrin β1 (*E* and *F*) and dystroglycan (*G* and *H*), were removed from underneath the podosomes when clusters mature. (Scale bar, 5 μm.)

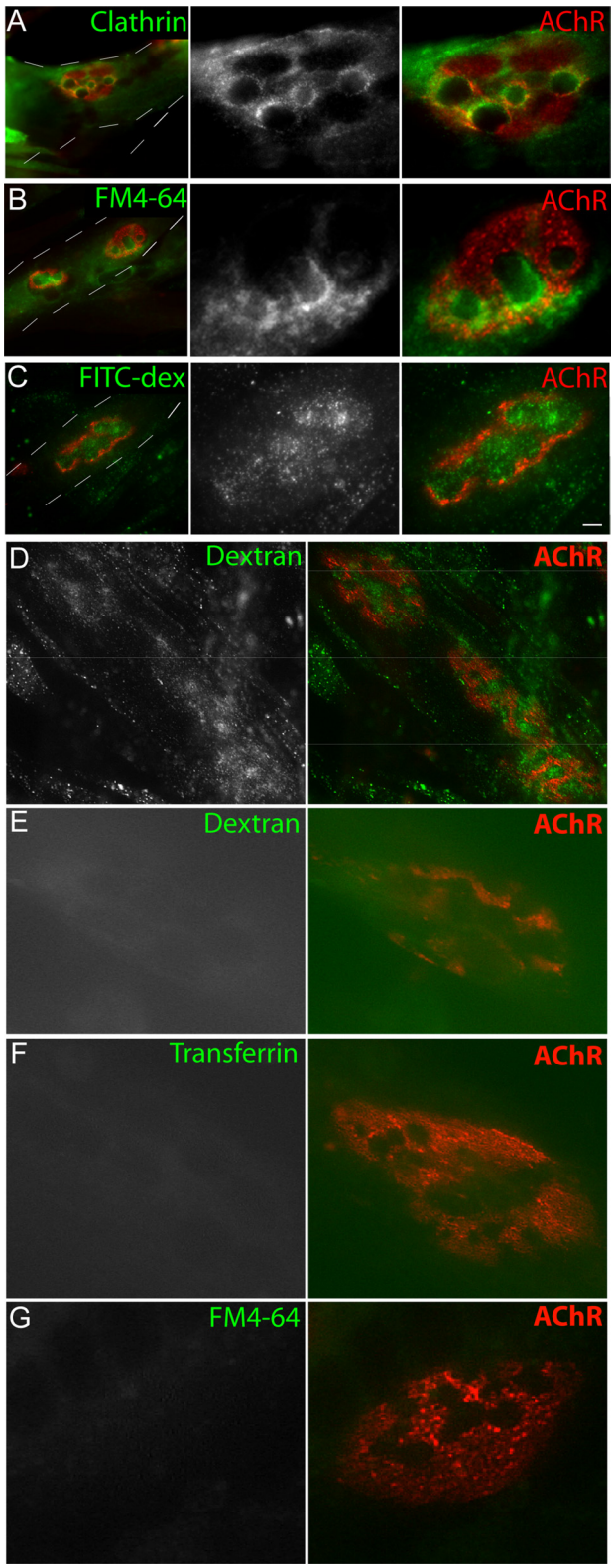

Fig. S6. Enhanced endocytosis associated with podosomes. (*A*) Endocytic machinery is concentrated around podosomes as shown for clathrin light chain. (*B* and *C*) Internalization of two fluorescently labeled endocytic tracers, FM4–64 (*B*) and low-molecular weight dextran (*C*) is enriched near podosomes. Endocytosis of fluorescently labeled tracers is blocked by incubation at low temperature. (*D*–*G*) C2C12 myotubes were incubated with indicated endocytic tracers at 37 °C (*D*) or on ice (after 15 min preincubation on ice): dextran (*D* and *E*), transferring (*F*), and FM4–64 (*G*). Uptake of the tracers was blocked at low temperature. (Scale bar, 5 μm.)

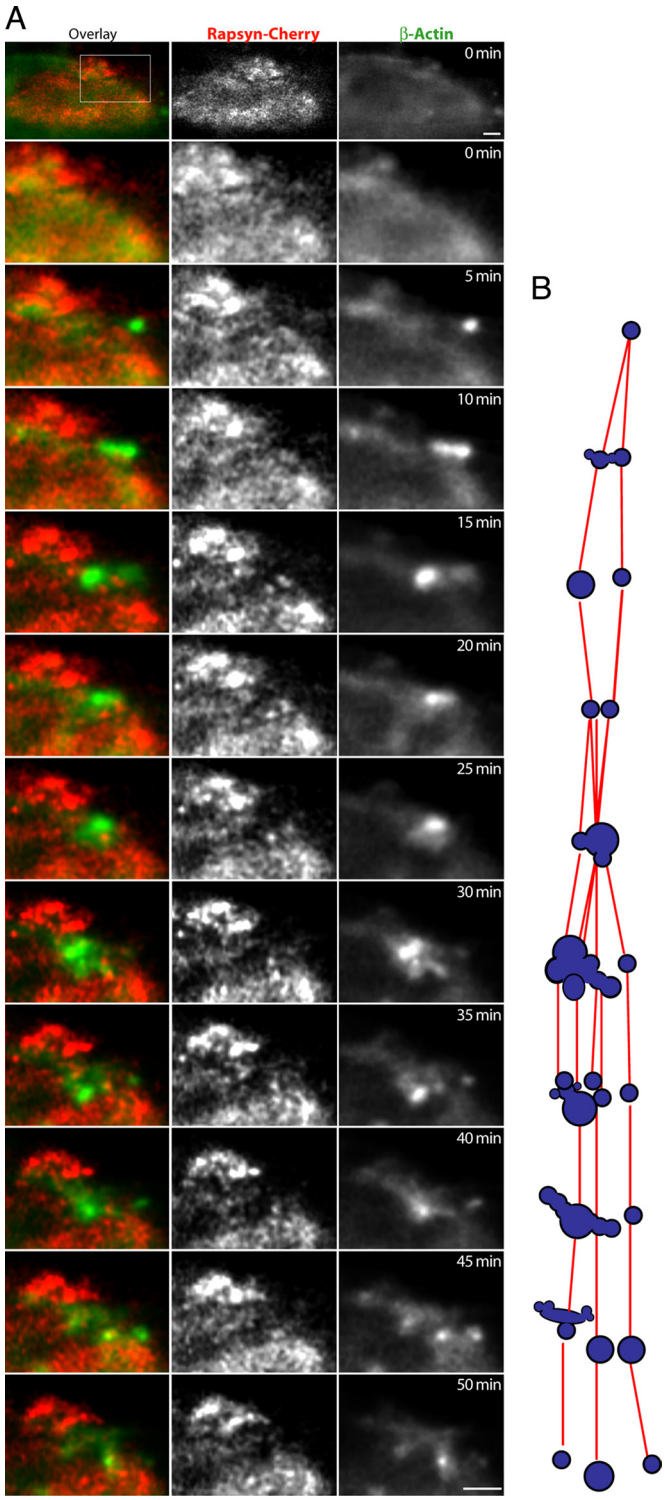

Fig. S7. Lateral dynamics of podosomes. (*A*) Sequence of images from a time-lapse experiment revealed lateral dynamics of synaptic podosomes. Low magnification image of the entire AChR cluster is shown in first row; square shows area magnified in next frames. Rapsyn-cherry was used to visualize the shape of the AChR cluster in this experiment. (*B*) Scheme showing position of podosomes in this experiment. Synaptic podosomes undergo fission and fusion, grow in size, and split into subunits that move laterally. (Scale bar, 5 μm.)

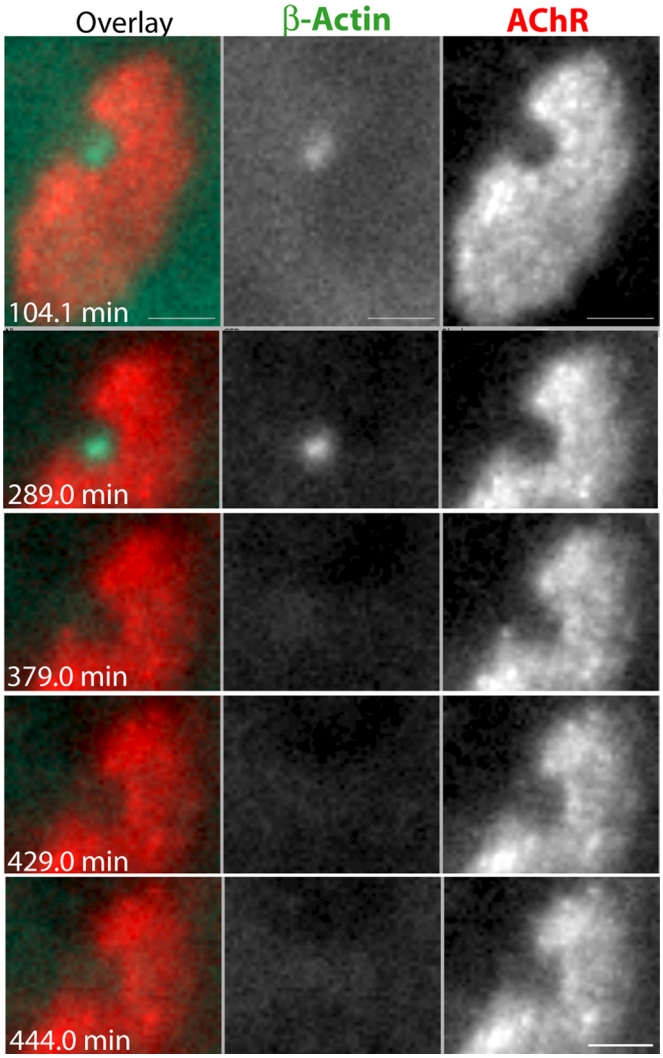

Fig. S8. Podosome dynamics prefigure alterations in the organization of AChRs. Disappearance of a podosome (after 289 min) is followed by appearance of AChRs in the perforation (at 444 min) and the edges of the perforation became blurry. (Scale bar, 5 μm.)

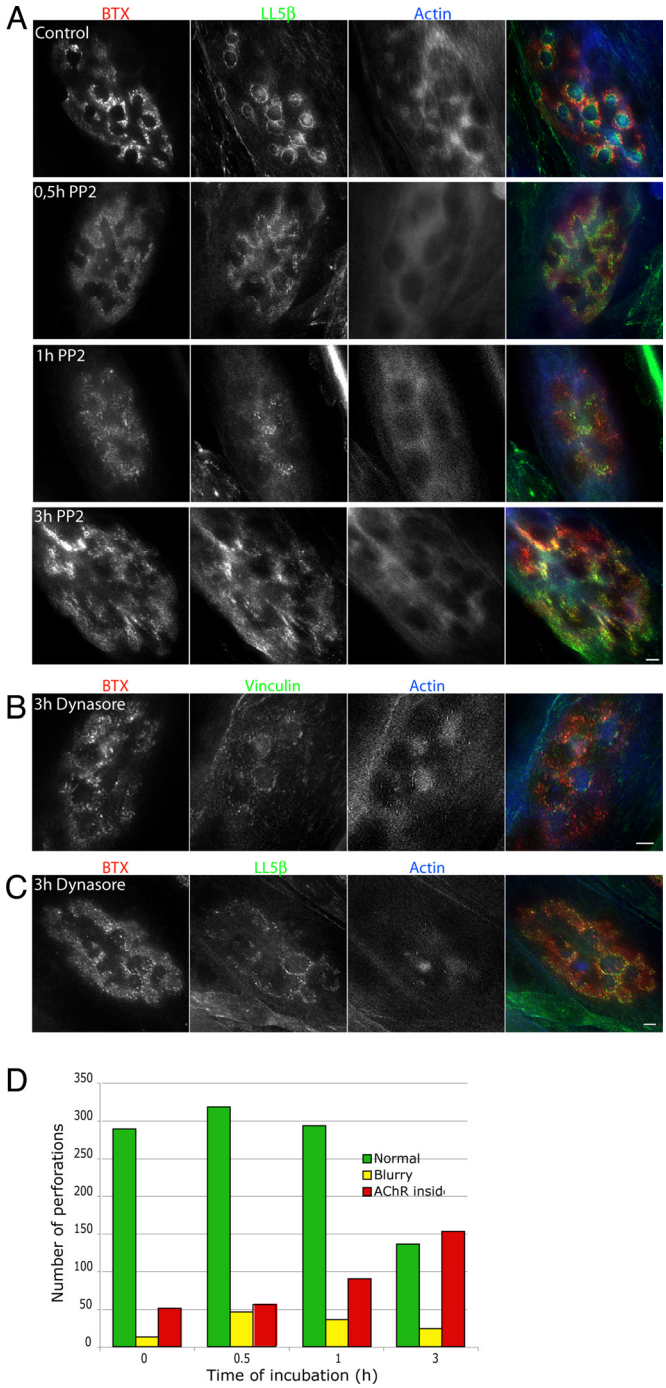

Fig. S9. Inhibitors of dynamin and Src family kinases affect organization of podosomes and AChRs within the cluster. (*A*) Incubation of C2C12 myotubes for 0.5–3 h with PP2 caused disassembly of podosome structures, as shown for actin and LL5β. (*B* and *C*) Treatment of cell culture with dynasore, led to decreased levels and diffuse distribution of podosome components, actin and vinculin (*B*), or LL5β (*C*). Disassembly of podosomes led to AChRs entry into perforations and loss of sharp edges. (*D*) Quantification of the effect of dynasore on the distribution of AChR at sites of cluster perforations. Graph shows measurements from a total of three cultures. (Scale bar, 5 μm.)

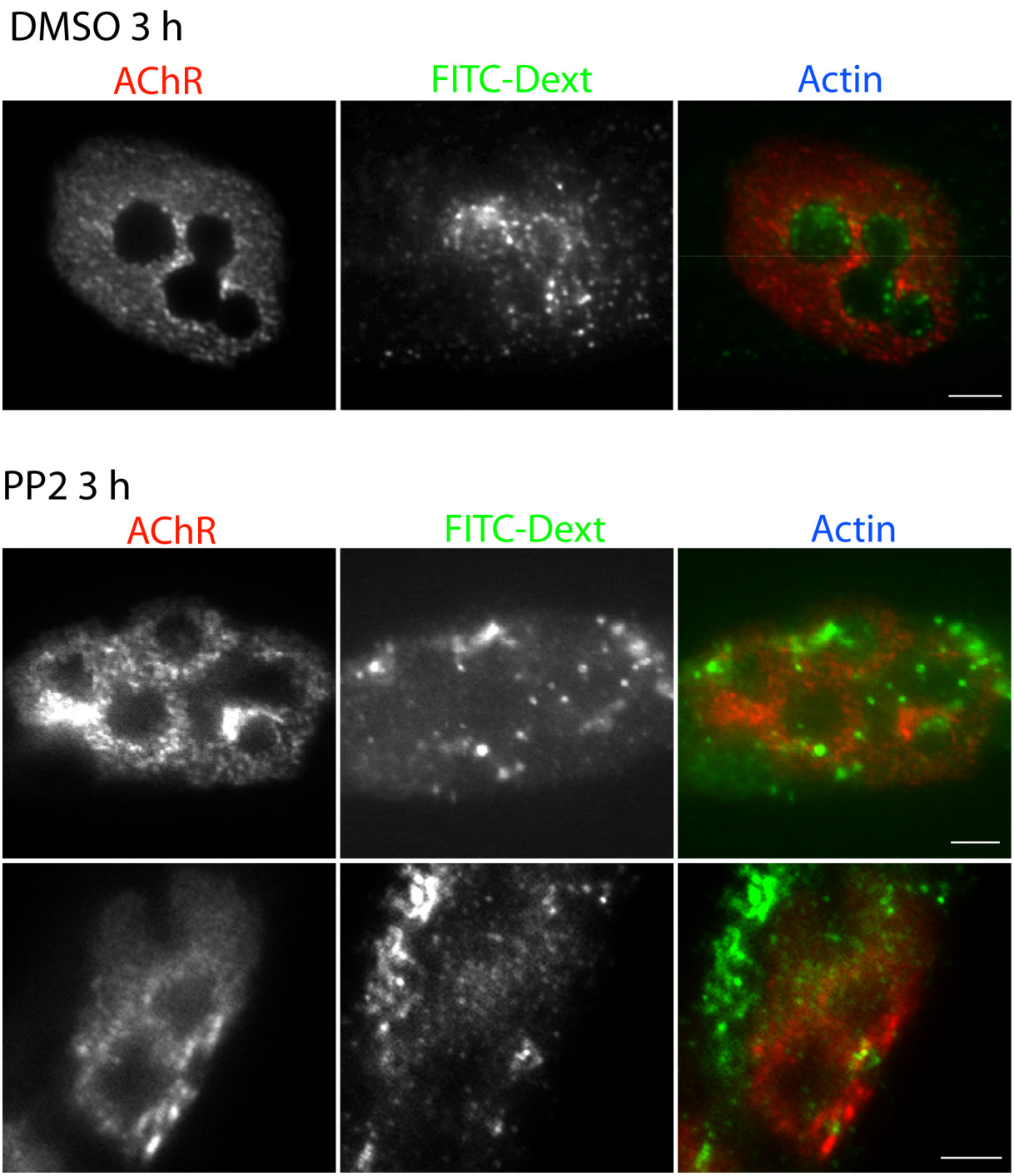

Fig. S10. Inhibitors of Src family kinases blocks enhanced endocytosis at the perforations in AChR clusters. In control experiments, podosome-containing perforations in AChR clusters are sites of enhaced endocytosis, as visualized by accumulated FITC-dextran labeling (see also Fig. S6). Preferential accumulation of dextran near the edges of perforations was abolished when cells were incubated with Src family kinase inhibitor PP2, which disrupts podosomes. (Scale bar, 5 μm.)